HHS Public Access

Author manuscript

Am J Surg Pathol. Author manuscript; available in PMC 2019 August 07.

Published in final edited form as:

Am J Surg Pathol. 2018 June ; 42(6): 767–777. doi:10.1097/PAS.0000000000001038.

Distinct Genomic Copy Number Alterations Distinguish Mucinous Tubular and Spindle Cell Carcinoma of the Kidney from Papillary Renal Cell Carcinoma with Overlapping Histologic Features

Qinghu Ren, MD, PhD[1], **Lu Wang, MD, PhD**[1], **Hikmat A. Al-Ahmadie, MD**[1], **Samson W. Fine, MD**[1], **Anuradha Gopalan, MD**[1], **Sahussapont J. Sirintrapun, MD**[1], **Satish K. Tickoo, MD**[1], **Victor E. Reuter, MD**[1], **Ying-Bei Chen, MD, PhD**[1,*]

[1]Department of Pathology, Memorial Sloan Kettering Cancer Center, New York, NY, USA

Abstract

Mucinous tubular and spindle cell carcinoma (MTSCC) of the kidney is a rare type of renal cell carcinoma that frequently exhibits histologic and immunophenotypic features overlapping with type 1 papillary renal cell carcinoma (PRCC). To clarify molecular attributes that can be used for this difficult differential diagnosis, we sought to delineate the genome-wide copy number alterations in tumors displaying classical histologic features of MTSCC in comparison to the solid variant of type 1 PRCC and indeterminate cases with overlapping histologic features. The study included 11 histologically typical MTSCC, 9 tumors with overlapping features between MTSCC and PRCC, and 6 cases of solid variant of type 1 PRCC. DNA samples extracted from macro- or microdissected tumor areas were analyzed for genome-wide copy number alterations using an SNP-array platform suitable for clinical archival material. All cases in the MTSCC group exhibited multiple chromosomal losses, most frequently involving chromosomes 1, 4, 6, 8, 9, 13, 14, 15 and 22, while lacking trisomy 7 or 17. In contrast, cases with overlapping morphologic features of MTSCC and PRCC predominantly showed multiple chromosomal gains, most frequently involving chromosomes 7, 16, 17, and 20, similar to the chromosomal alteration pattern that was seen in the solid variant of type 1 PRCC cases. Morphologic comparison of these molecularly characterized tumors identified histologic features that help to distinguish MTSCC from PRCC, but immunohistochemical profiles of these tumors remained overlapping, including a marker for Hippo-YAP signaling. Characteristic patterns of genome-wide copy number alterations strongly support MTSCC and PRCC as distinct entities despite their immunohistochemical and certain morphologic overlap, and help define histologic features useful for the classification of questionable cases.

Keywords

mucinous tubular and spindle cell carcinoma; papillary renal cell carcinoma; chromosomal aberration; SNP array; Hippo-YAP signaling

[*]Corresponding Author: Ying-Bei Chen, MD, PhD, Assistant Attending Pathologist, Department of Pathology, Memorial Sloan Kettering Cancer Center, New York, NY 10065, Tel: (212) 639-6338, Fax: (212) 717-3203, cheny@mskcc.org.

Disclosures: The authors have no conflicts of interest to disclose.

Introduction

Mucinous tubular and spindle cell carcinoma (MTSCC) of kidney is a distinct subtype of renal cell carcinoma (RCC) recognized in the recent World Health Organization (WHO) classifications of tumors.[1, 2] Classically, this subtype of RCC shows tightly packed elongated, branching tubules lined by low-grade cuboidal cells merging with bland spindle cell elements in a mucinous or myxoid stroma.[3–7] In most case series, it occurs more frequently in females (F:M = 3–4:1) and is associated with indolent clinical behavior.[4–11] The morphological spectrum of MTSCC, however, can include some unusual features, such as spindle cell-predominant, tubular epithelial component-predominant, mucin-poor, focal papillations or rarely well-formed papillae, necrosis, and clear cell changes.[11–13] Occasional cases displaying high-grade nuclear features, sarcomatoid differentiation, and lymph node or distant metastasis have also been reported.[10, 14–23]

The main differential diagnostic consideration for MTSCC is type 1 papillary RCC (PRCC) that has predominantly solid or tubular architectural patterns or contains low-grade spindle cell areas.[24, 25] Immunohistochemical profiles of these tumors show significant overlap, with a large majority of cases exhibiting immunoreactivity to CK7, AMACR, and EMA.[8, 9] At the genomic level, Rakozy et al. have reported a unique pattern of losses of chromosomes 1, 4, 6, 8, 9, 13, 14, 15, and 22 in all six MTSCC tumors analyzed by comparative genome hybridization (CGH) and loss of heterozygosity (LOH) analyses.[6] Similar chromosome aberrations were subsequently identified by other studies.[5, 10, 26, 27] However, some cases in these prior studies were also reported to harbor multiple chromosomal gains, including 7, 11, 16, 17, and 20, the pattern more characteristically observed in PRCC. [5, 26, 27] In parallel, some studies have found fluorescence in situ hybridization (FISH) analysis for trisomies 7 and 17 helpful in this differential diagnosis,[25, 28] while others reported inconsistent findings. [29, 30] On the other hand, studies of the solid variant of PRCC and PRCC with low-grade spindle cell foci examined trisomies 7 and 17 by FISH analysis, with most identifying the presence of trisomy 7 and/or trisomy 17.[24, 25, 30–33]

Using whole-exome sequencing, a very recent study of MTSCC with classic morphology revealed monosomy of chromosomes 1, 6, 9, 14, 15, and 22 in 100% of 22 cases, and frequent loss of chromosomes 4, 8, and 13 in 80–90% of cases.[34] The study also suggested biallelic alteration and dysregulation of Hippo pathway as a common molecular basis for the disease. Meanwhile, type 1 PRCC in The Cancer Genome Atlas (TCGA) study predominantly showed multiple chromosomal gains, including nearly universal gains of chromosomes 7 and 17 and less frequent gain of chromosomes 2, 3, 12, 16, and 20.[35] While these new molecular studies support MTSCC and type 1 PRCC as distinct entities, it remains unclear whether MTSCC is molecularly distinct from PRCC variants that histologically closely mimic MTSCC, and how pathologists should practically approach cases with overlapping histologic features.

In this study, we performed genome-wide copy number and allelic imbalance analysis of MTSCC, solid variant of type 1 PRCC, and cases with overlapping histologic features using a high-resolution SNP-array platform that is suitable for clinical archival material. For

tumors with intratumoral morphological heterogeneity, we specifically investigated morphologically distinct areas. Based on findings from this molecular analysis, we re-evaluated the morphologic features of tumors in different diagnostic groups and assessed the utility of potential immunohistochemical tests including a marker for the dysregulated Hippo-YAP pathway.

Materials and methods

Case selection and histologic review

The study included 26 retrospectively selected patients who underwent radical or partial nephrectomy at our institution during 2006–2016 with a diagnosis of MTSCC, PRCC (type 1) or an indeterminate histologic subtype with diagnostic comments indicating overlapping features between MTSCC and PRCC. All archival material from these cases were retrieved and re-reviewed, and cases were divided into 3 groups based on histologic features. The MTSCC group included 11 cases with the typical morphologic appearance of MTSCC, exhibiting an admixture of tubules, spindle cells, and mucinous stroma in variable proportions as well as low grade nuclei. The PRCC control group included 6 cases of type 1 PRCC, solid variant, which predominantly consisted of solid growth of tumors cells forming micronodules, abortive papillae or ill-defined tubules.[24] The third group included 9 cases of RCC with overlapping features between MTSCC and PRCC. All clinical data were collected through chart review. Detailed histologic characteristics were recorded for each tumor, which included the percentages of various growth patterns such as elongated tubules, short tubules, spindle cells, solid sheet of cells, micronodules or abortive papillae (without fibrovascular cores), and well-formed papillae with fibrovascular cores, as well as the presence or absence of fibrous capsule/pseudocapsule, mucin, or foamy macrophages. The 7th edition AJCC TNM system was used for tumor staging. The study was approved by our Institutional Review Board. All H&E slides were reviewed to select representative areas of the tumors for the SNP array analysis.

Immunohistochemistry

Immunohistochemistry was conducted in 5 μm formalin-fixed paraffin-embedded (FFPE) whole tissue sections. Staining for CK7 (clone OV-TL 12/30, DAKO, 1:800), AMACR (clone 12H4, Zeta Corp, 1:100), CD10 (clone SP67, Ventana), EMA (clone E29, Ventana), CD15 (clone MMA, Ventana) and Pax8 (Proteintech, 1:100) was performed using a BenchMark XT automated system (Ventana, Tucson, AZ). Staining for YAP/TAZ (D24E4, Cell Signaling Technology, 1:50) was performed using an automated Ventana Discovery system (Ventana). Immunostaining scores (H-scores) for YAP/TAZ nuclear staining were determined as [H= intensity (0–3) x percentage of positive cells (1–100)].

DNA sample preparation

DNA samples were extracted from FFPE tissue using QIAamp DNA FFPE tissue kit according to the manufacturer's standard protocol (Qiagen, Valencia, CA). For tumors with intratumoral histologic heterogeneity, representative areas were macro- or microdissected for DNA extraction. Concentration and quality of the sample were assessed with Qubit 2.0

Fluorometer (Life Technologies, Carlsbad, CA) and gel electrophoresis using reference DNA as a control.

High-resolution SNP array analysis

Genome-wide DNA copy number alterations and allelic imbalances were analyzed by SNP-array using Affymetrix OncoScan FFPE Assay (Affymetrix, Santa Clara, CA) according to the manufacturer's guidelines. Briefly, genomic DNA samples (80 ng input) were hybridized to MIP probes followed by gap filling with AT/GC. After removing the unligated probes through exonuclease treatment, the cleavage enzyme was added to linearize the gap-filled circular MIP probes. This was followed by amplification, enrichment, digestion, and hybridization. The hybridized array was washed, stained and scanned through GENECHIP Scanner-7G (Affymetrix). Assay data were analyzed by OncoScan Console software (Affymetrix) and OncoScan Nexus Express software (BioDiscovery, El Segundo, CA) using Affymetrix TuScan algorithm. All array data were also manually reviewed for subtle alterations not automatically detected by the software.

Results

Clinicopathologic characteristics

The clinicopathologic features of 26 cases in the 3 diagnostic groups, including MTSCC (n = 11), PRCC, solid variant (n = 6) and indeterminate cases with overlapping features (IND, n = 9), are summarized in Table 1. There was a female predilection (4.5:1) in the MTSCC group which is consistent with the previous literature[2], and distinct from the male predominance observed in the other two groups. At the time of nephrectomy, almost all tumors in the cohort were organ-confined without perirenal adipose tissue or renal vein invasion; one case in the IND group invaded into perinephric fat. There was no significant difference between tumor size among the 3 groups. No lymph node involvement was identified in cases submitted to regional lymph node dissection (n = 6). Papillary adenomas were identified in 4 cases, including 1 MTSCC and 3 IND cases. The median follow-up time for the entire cohort (n = 26) was 43 months (range 3–120 months). During follow-up, one patient from the IND group developed lymph node and distant metastasis, 5 years post-surgery. This patient was alive with disease at last follow-up (120 months). All other patients were alive and without evidence of recurrence or progression.

Morphologic spectrum

The histologic features of all cases are summarized in Table 2. All tumors were relatively circumscribed, with (n = 14) or without (n = 12) a fibrous capsule. Within the MTSCC group (Fig. 1), 7 of 11 (64%) cases exhibited apparent stromal mucin whereas 4 cases (36%) were mucin-poor. Elongated, branching tubules were found to be the dominant component in 6 of 11 (55%) cases, and other patterns included short tubules, spindle cells, or solid sheets of tumor cells (Fig. 1A–1D). The majority of cases (10 of 11, 91%) exhibited focal (5–10%) micronodules formed by whorled tubules (Fig. 1E–1F), and 4 cases (36%) contained rare foci of small papillae with fibrous cores (Fig. 1D). Foamy macrophages were identified in 7 of 11 (64%) cases, mostly as scattered small foci within stroma in a background of tubular or solid tumor growth (Fig. 1B).

In comparison, within the PRCC group, micronodules or abortive papillae (Fig. 2A) were the most prevalent growth pattern in 4 of 6 (67%) of cases, whereas elongated tubules were either absent or as a minor component (5–20%). Short or ill-formed tubules, solid sheets, and low-grade spindle cells were also present (Fig. 2B–2D). Three cases had distinct areas (10–20% of tumor) of well-formed papillae with type 1 PRCC histologic features (Fig. 2B). Stromal mucin was absent in all 6 cases. Abundant stromal foamy macrophages were found in 4 of 6 (67%) cases.

The 9 cases in the IND group could be separated into two subsets based on their morphologic features. Three cases (33%, IND5, IND6, and IND9) had distinct papillary regions with well-formed papillae of type 1 PRCC, yet also contained separate large areas displaying MTSCC-like features with intermixed tubules, solid sheets or spindle cells (Fig. 3A–3B). Two of these 3 cases showed stromal mucin in the MTSCC-like regions. The remaining 6 cases (67%) had tubular, solid, and spindle cell components as well as micronodules or abortive papillae intermixed intimately (Fig. 3C–3E). When compared to the PRCC group, this subset of IND cases had a higher proportion of elongated tubules; compared to MTSCC, they showed an increased presence of micronodules or abortive papillae. Mucin was readily identified in 2 of 6 cases but was mainly luminal in one case (Fig. 3D). Additionally, two of these 6 cases showed well-developed branching papillae within the micronodules (Fig. 3F).

Genome-wide copy number alterations detected in MTSCC, PRCC and IND groups

From the 26 cases, a total of 33 DNA samples were assessed by high-resolution SNP array (Fig. 4). In 7 cases (1 MTSCC, 1 PRCC, and 5 INDs), two independent DNA samples from areas with different histologic features were analyzed. The 12 samples from 11 MTSCC cases showed a consistent pattern of multiple chromosomal copy number losses, most frequently involving chromosomes 1 (100%), 4 (83%), 6 (100%), 8 (92%), 9 (83%), 13 (83%), 14 (100%), 15 (100%), and 22 (100%) (Fig. 4A and 4C). Other less frequent chromosomal losses included 18 (50%), 11 or 11q (25%), and 10 (17%). The two relatively distinct areas in MTSCC10, intermixed tubular, spindled and solid sheets of cells versus elongated tubules forming micronodules, exhibited very similar chromosomal copy alterations (Fig. 4C).

On the other hand, the 7 samples from 6 PRCC cases exhibited a consistently distinct pattern that predominantly included chromosomal gains of 7 (100%), 16 (71%), 17 (100%), and 20 (71%). Other chromosomal gains involved 3, 10, 12, and 21, and occurred at much lower frequency (Fig. 4B and 4C). Infrequent chromosomal losses were seen in two cases (PRCC3 and 6), but with patterns different from MTSCC. In PRCC4 where two distinct areas were examined, the area dominated by micronodules/abortive papillae (Fig. 2A) had similar copy number changes as the area with a solid growth pattern and spindle cells.

Interestingly, all 14 samples from 9 cases in the IND group with overlapping histologic features showed multiple chromosomal gains that most frequently involved 7 (79%), 16 (57%), 17 (100%), and 20 (93%), a pattern similar to the PRCC group (Fig. 4C). None of the samples in the IND group exhibited the pattern of chromosomal losses observed in the MTSCC group, including the areas with the MTSCC-like appearance. Paired samples from

the same tumor generally displayed very similar copy number alterations. The most divergence of paired samples was seen with case IND9: while sharing gains of 17 and 20, the papillary area (IND9_1) and solid area (IND9_2) had other distinct gains involving different chromosomes. Overall, despite the morphologic ambiguity, the copy number alterations detected in these IND cases strongly support their classification as PRCC.

Morphologic features helpful for distinguishing MTSCC from PRCC

As the SNP array data confirmed our initial grouping of MTSCC and PRCC cases in the study and further classified all our IND cases as PRCC, we reassessed the histologic features of MTSCC cases (n = 11) in comparison to those of the molecularly-defined PRCC cases (n = 15). While the presence or absence of capsule/pseudocapsule, proportion of various architectural patterns, mucin, or foamy macrophages could not definitively distinguish these two entities in this cohort (Table 2), we identified 3 distinct morphologic features that were present in PRCC but not MTSCC cases (Table 3).

The first feature was the presence of a distinct area of well-formed, type 1 papillae (Figs. 2B and 3A). In comparison, the rare papillae seen in MTSCC mostly appeared to be isolated small papillations with minimal fibrous cores scattered in a background of tubules with twisted lumina or papillary infolding (Fig. 1D). A second feature was low-grade spindle cell foci previously described in PRCC[25], which showed spindled tumor cells lining angulated, curvilinear tubules with irregular and “shaggy” lumina (Fig. 2D). Conversely, the lumina of tubules in tightly packed tubular and spindle cell areas of MTSCC were typically smoother (Fig. 1B–C). Each of these two morphologic features existed in 40% (n=6) of the PRCC analyzed and showed a significant correlation with the PRCC diagnosis ($p < 0.05$).

Lastly, we only observed micronodules encompassing small branching papillae that clearly contained fibrovascular cores (Fig. 3F) in PRCC cases, although this feature was only prevalent in 2 of 15 PRCC cases in the study. In the remaining cases of PRCC, while there might be subtle morphologic differences between the micronodules or abortive papillae (Fig. 2A and 3C) versus those seen in MTSCC (compact arrangement of whorled tubules, Fig. 1E–F), they all lacked well-formed fibrovascular cores and could be very difficult to distinguish.

Immunohistochemical features

The immunohistochemical features of tumors in this study are summarized in Table 4. CD10 was largely negative (7/10, 70%) in the MTSCC group, whereas 69% of PRCC cases showed at least focal immunoreactivity. However, 4 of the 13 (31%) tested PRCC cases, all from the IND group, also showed negative staining for CD10, indicating the limited utility of this marker in cases with equivocal histologic features. Consonant with previous literature,[8, 9] the results of CK7, AMACR, PAX8, EMA, and CD15 were similar between MTSCC and PRCC groups.

Given the recent implication of dysregulated Hippo pathway in MTSCC,[34] we examined the expression of Yes-associated protein (YAP) and transcriptional activator with PDZ-binding domain (TAZ), two transcription co-activators that are the major downstream effectors of the Hippo pathway.[36] Using an antibody detecting the total YAP and TAZ proteins, we tested

the utility of this marker in the differential diagnosis of MTSCC from PRCC with overlapping histologic features. There was no significant difference in the nuclear expression of YAP/TAZ detected between molecularly-defined MTSCC and PRCC cases (Fig. 5). The mean H-score was 207 (range 130–280) in the MTSCC group versus 232 (range 170–280) in the PRCC group.

Discussion

Cases with morphologic features of MTSCC were originally reported in 1997 and grouped under the descriptive name of “low-grade collecting duct carcinoma” together with what later proved to be tubulocystic carcinomas.[37] As a specific entity, MTSCC was designated as the official name in the 2004 WHO classification system to acknowledge its characteristic morphologic features collectively described in a few early studies.[3–7] However, it was soon appreciated that MTSCC and type 1 PRCC, particularly the solid variant, share significant morphologic and immunohistochemical overlap.[8, 11] The accurate classification of these two entities for cases with atypical or overlapping features has remained a difficult diagnostic challenge.

In this study, we investigated genome-wide copy number alterations in MTSCC, solid variant of type 1 PRCC, and indeterminate cases with overlapping histologic features to elucidate molecular attributes that can be used in this differential diagnosis. We demonstrate that MTSCC and PRCC exhibit distinct chromosome alteration patterns that clearly separate the two entities, and that the chromosomal alterations revealed by a SNP-array platform are able to definitively resolve the classification of indeterminate cases with overlapping histologic features. Since this array-based technology has been fully adapted for limited FFPE material and is increasingly being used in clinical laboratories, it can serve as a powerful ancillary tool for this challenging pathologic distinction.

Our results showed that all MTSCC cases exhibit multiple chromosomal losses frequently involving chromosomes 1, 4, 6, 8, 9, 13, 14, 15 and 22 while lacking trisomy 7/17, whereas solid variant of type 1 PRCC cases show multiple chromosomal gains most frequently involving chromosomes 7, 16, 17, and 20. These findings corroborate results from a recent whole-exome sequencing study of MTSCC with classic morphology and the comprehensive genomic characterization of type 1 cases in the TCGA PRCC study,[34, 35] and support the notion that MTSCC and type 1 PRCC harbor distinct and characteristic chromosomal copy number alterations. One unique feature of our study is that we examined intratumoral morphologic heterogeneity and showed that the overall patterns of chromosomal copy number alteration are identical or very similar among morphologically distinct areas within a given tumor.

Another important feature of our study is that we focused on morphologically ambiguous cases and investigated in detail the morphologic and molecular features of cases with overlapping features of MTSCC and PRCC. It is interesting to note that 3 of the 161 cases included in the TCGA PRCC cohort were found to have the MTSCC-type multiple chromosomal losses, while lacking characteristic genetic changes of type 1 PRCC.[34] This reiterates the difficulty in distinguishing these two entities based on routine histologic and

immunohistologic criteria. Prior reports on genomic findings in RCC with overlapping histologic features of MTSCC and PRCC are largely lacking. One recent study included 6 such cases and found one case showing MTSCC-type multiple chromosomal losses, 2 with PRCC-type multiple gains, and 1 case without any abnormality, although details on morphologic and molecular correlation were not provided.[38] In this study, we found that all cases from our IND group harbored copy number alterations characteristic of PRCC. Given the morphologic spectrum seen in these PRCC cases with IND histology, our results emphasize the fact that areas closely resembling MTSCC can exist in PRCC; such areas include intermixed tubules and solid sheets of epithelioid or spindle cells, and even the presence of stromal mucin.

Taking advantage of these molecularly-defined cohorts of MTSCC and PRCC, we reassessed the histologic features of all cases and found that the presence of a distinct, well-formed type 1 papillary area (vs. isolated small papillations in MTSCC), or spindled cell-lined, angulated/curvilinear tubules with irregular and “shaggy” lumina, as originally described by Argani et al[25], correlated with a diagnosis of PRCC. Another less frequent histologic feature, micronodules encompassing small branching papillae that clearly contained well-defined fibrovascular cores (Fig. 3F), was also only found in PRCC. As these features were not identified in MTSCC cases, they potentially serve as more definitive histologic clues during pathologic evaluation, particularly for cases with overlapping features. However, given the relatively small size of this cohort, further studies in larger independent cohorts are needed to better assess their utility. Additionally, it needs to be emphasized that these histologic criteria should be applied in the appropriate histologic context, and that they are not intended for cases with differential diagnoses extending beyond the scope of MTSCC and type 1 PRCC.

The immunohistochemistry results of this study are in line with the previous studies. Among the routine immunohistochemical markers, although CD10 was negative in 70% of MTSCC cases yet showed at least some immunoreactivity in approximately 70% of PRCC, its utility as a diagnostic marker is limited as 30% of PRCCs in this cohort were also negative. Hippo pathway dysregulation has recently been suggested as a common molecular basis for MTSCC, with up to 90% cases exhibiting increased nuclear YAP1 protein expression in one study.[34] While we indeed found relatively high nuclear expression of YAP/TAZ in MTSCC cases, the levels of YAP/TAZ in PRCCs of this cohort were also high and comparable to MTSCC. Consistent with Hippo pathway activation that has also been identified in RCC of other histologic subtypes, such as some “type 2” PRCC and unclassified RCC[35, 39], our finding suggests that markers for this pathway have limited value for the differential diagnosis of MTSCC from its PRCC mimics.

Although the copy number alterations identified in our study support FISH analysis of trisomies 7 and 17 as a useful ancillary tool for the distinction of PRCC and MTSCC, false positive or false negative results in FISH trisomy analysis due to difficulties in interpreting fluorescence signals or setting correct thresholds are not rare. Additionally, relying on a negative result for trisomy 7 or 17 to diagnose MTSCC can be misleading, particularly if the differential diagnosis for a given case includes other entities. For example, in a case that was reported as an MTSCC with extensive papillary architecture in a patient with end-stage

kidney disease based on the negative result for FISH trisomy 7 or 17, the diagnosis might have benefited from further studies using FISH probes for multiple chromosomes or genome-wide copy number analysis by SNP or CGH array.[40] In our experience, the SNP-array based assay can render a high-resolution genome-wide characterization of copy number alterations, including detecting copy-neutral LOH, using routinely processed, limited clinical FFPE samples. We also believe that compared to FISH, SNP array shows better sensitivity and specificity for classifying MTSCC cases and distinguishing them from its histologic mimics.

While the MTSCC cases in our cohort exhibited low nuclear grade, it is also worth noting that recent studies of MTSCC with high nuclear grade (Fuhrman grade 3 or WHO/ISUP nucleolar grade 3) identified copy number changes similar to classic MTSCC.[20, 23] Utilizing the same SNP array platform as in this study, we have analyzed 7 high-grade MTSCC cases and identified multiple chromosomal losses similar to the pattern described here.[23] However, in cases with more complex high-grade features or sarcomatoid change, chromosomal gains or additional LOH may be detected, although data in this regard are very limited.[14, 23]

In conclusion, MTSCC exhibits a distinct copy number alteration pattern, most frequently monosomy of 1, 4, 6, 8, 9, 13, 14, 15, and 22, whereas solid variant of PRCC and other PRCC with overlapping histologic features are characterized by chromosomal gains of 7, 17 and 20. For cases with mixed or overlapping features of MTSCC and PRCC that are difficult to classify, SNP array can serve as a very powerful ancillary tool for the differential diagnosis. The presence of classic type 1 papillary area or spindled cells lining angulated, curvilinear tubules with irregular and “shaggy” lumina favors a diagnosis of PRCC, and the utility of these relatively distinctive histologic features in this differential diagnosis needs to be confirmed by additional studies.

Acknowledgments

The work received funding from Cycle for Survival of Memorial Sloan Kettering Cancer Center (Y-B.Chen). L. Wang, H.A. Al-Ahmadie, S.W. Fine, A. Gopalan, S.J. Sirintrapun, S.K. Tickoo, V.E. Reuter, and Y-B. Chen were funded in part by an NIH/NCI Cancer Center Support Grant (P30 CA008748).

References

1. Eble JN, Sauter G, Epstein JI, et al., eds. WHO Classification of Tumours of the Urinary System and Male Genital Organs (3rd edition). Lyon: IARC Press; 2004.
2. Moch H, Humphrey PA, Ulbright TM, et al., eds. WHO Classification of Tumours of the Urinary System and Male Genital Organs (4th edition). Lyon: IARC; 2016.
3. Srigley JR, Eble JN, Grignon DJ, et al. Unusual renal cell carcinoma (RCC) with prominent spindle cell change possibly related to the loop of Henle. Mod Pathol. 1999;12:107A.
4. Parwani AV, Husain AN, Epstein JI, et al. Low-grade myxoid renal epithelial neoplasms with distal nephron differentiation. Hum Pathol. 2001;32:506–512. [PubMed: 11381369]
5. Srigley JKL, Reuter V, Amin M, Grignon D, Eble J, Weber A, Moch H. Phenotypic, molecular and ultrastructural studies of a novel low grade renal epithelial neoplasm possibly related to the loop of Henle. Mod Pathol. 2002;15:182A.
6. Rakozy C, Schmahl GE, Bogner S, et al. Low-grade tubular-mucinous renal neoplasms: morphologic, immunohistochemical, and genetic features. Mod Pathol. 2002;15:1162–1171. [PubMed: 12429795]

7. Hes O, Hora M, Perez-Montiel DM, et al. Spindle and cuboidal renal cell carcinoma, a tumour having frequent association with nephrolithiasis: report of 11 cases including a case with hybrid conventional renal cell carcinoma/spindle and cuboidal renal cell carcinoma components. Histopathology. 2002;41:549–555. [PubMed: 12460208]
8. Paner GP, Srigley JR, Radhakrishnan A, et al. Immunohistochemical analysis of mucinous tubular and spindle cell carcinoma and papillary renal cell carcinoma of the kidney: significant immunophenotypic overlap warrants diagnostic caution. Am J Surg Pathol. 2006;30:13–19. [PubMed: 16330937]
9. Shen SS, Ro JY, Tamboli P, et al. Mucinous tubular and spindle cell carcinoma of kidney is probably a variant of papillary renal cell carcinoma with spindle cell features. Ann Diagn Pathol. 2007;11:13–21. [PubMed: 17240302]
10. Ferlicot S, Allory Y, Comperat E, et al. Mucinous tubular and spindle cell carcinoma: a report of 15 cases and a review of the literature. Virchows Arch. 2005;447:978–983. [PubMed: 16231179]
11. Fine SW, Argani P, DeMarzo AM, et al. Expanding the histologic spectrum of mucinous tubular and spindle cell carcinoma of the kidney. Am J Surg Pathol. 2006;30:1554–1560. [PubMed: 17122511]
12. Farghaly H Mucin poor mucinous tubular and spindle cell carcinoma of the kidney, with nonclassic morphologic variant of spindle cell predominance and psammomatous calcification. Ann Diagn Pathol. 2012;16:59–62. [PubMed: 21310639]
13. Cao W, Huang B, Fei X, et al. Clear cell changes in mucinous tubular and spindle cell carcinoma: cytoplasmic pallor/clearing within tubules, vacuoles or hybrid conventional clear cell carcinoma of kidney? Int J Clin Exp Pathol. 2014;7:4350–4358. [PubMed: 25120820]
14. Dhillon J, Amin MB, Selbs E, et al. Mucinous tubular and spindle cell carcinoma of the kidney with sarcomatoid change. Am J Surg Pathol. 2009;33:44–49. [PubMed: 18941398]
15. Simon RA, di Sant'agnese PA, Palapattu GS, et al. Mucinous tubular and spindle cell carcinoma of the kidney with sarcomatoid differentiation. Int J Clin Exp Pathol. 2008;1:180–184. [PubMed: 18784804]
16. Pillay N, Ramdial PK, Cooper K, et al. Mucinous tubular and spindle cell carcinoma with aggressive histomorphology - a sarcomatoid variant. Hum Pathol. 2008;39:966–969. [PubMed: 18400251]
17. Bulimbasic S, Ljubanovic D, Sima R, et al. Aggressive high-grade mucinous tubular and spindle cell carcinoma. Hum Pathol. 2009;40:906–907. [PubMed: 19442792]
18. Arafah M, Zaidi SN. Mucinous tubular and spindle cell carcinoma of the kidney with sarcomatoid transformation. Saudi J Kidney Dis Transpl. 2013;24:557–560. [PubMed: 23640631]
19. Kenney PA, Vikram R, Prasad SR, et al. Mucinous tubular and spindle cell carcinoma (MTSCC) of the kidney: a detailed study of radiological, pathological and clinical outcomes. BJU Int. 2015;116:85–92. [PubMed: 25395040]
20. Kuroda N, Hes O, Michal M, et al. Mucinous tubular and spindle cell carcinoma with Fuhrman nuclear grade 3: A histological, immunohistochemical, ultrastructural and FISH study. Histol Histopathol. 2008;23:1517–1523. [PubMed: 18830937]
21. Ursani NA, Robertson AR, Schieman SM, et al. Mucinous tubular and spindle cell carcinoma of kidney without sarcomatoid change showing metastases to liver and retroperitoneal lymph node. Hum Pathol. 2011;42:444–448. [PubMed: 21194728]
22. Qi XL, Zhao M, He XL, et al. Mucin-poor mucinous tubular and spindle cell renal cell carcinoma with sarcomatoid transformation and multiple metastases: report of a unique case and review of literature. Int J Clin Exp Pathol. 2016;9:2451–2458.
23. Sadimin ET, Chen YB, Wang L, et al. Chromosomal abnormalities of high-grade mucinous tubular and spindle cell carcinoma of the kidney. Histopathology. 2017;71:719–724. [PubMed: 28656700]
24. Renshaw AA, Zhang H, Corless CL, et al. Solid variants of papillary (chromophil) renal cell carcinoma: clinicopathologic and genetic features. Am J Surg Pathol. 1997;21:1203–1209. [PubMed: 9331293]
25. Argani P, Netto GJ, Parwani AV. Papillary renal cell carcinoma with low-grade spindle cell foci - A mimic of mucinous tubular and spindle cell carcinoma. Am J Surg Pathol. 2008;32:1353–1359. [PubMed: 18670354]

26. Brandal P, Lie AK, Bassarova A, et al. Genomic aberrations in mucinous tubular and spindle cell renal cell carcinomas. Mod Pathol. 2006;19:186–194. [PubMed: 16258504]
27. Weber A, Srigley J, Moch H. [Mucinous spindle cell carcinoma of the kidney. A molecular analysis]. Der Pathologe 2003;24:453–459. [PubMed: 14605851]
28. Cossu-Rocca P, Eble JN, Delahunt B, et al. Renal mucinous tubular and spindle carcinoma lacks the gains of chromosomes 7 and 17 and losses of chromosome Y that are prevalent in papillary renal cell carcinoma. Mod Pathol. 2006;19:488–493. [PubMed: 16554730]
29. Okon K, Klimkowska A, Pawelec A, et al. Immunophenotype and cytogenetics of mucinous tubular and spindle cell carcinoma of the kidney. Pol J Pathol. 2007;58:227–233. [PubMed: 18459456]
30. Zhang Y, Yong X, Wu Q, et al. Mucinous tubular and spindle cell carcinoma and solid variant papillary renal cell carcinoma: a clinicopathologic comparative analysis of four cases with similar molecular genetics datum. Diagn Pathol. 2014;9:194. [PubMed: 25476569]
31. Cantley R, Gattuso P, Cimbaluk D. Solid variant of papillary renal cell carcinoma with spindle cell and tubular components. Arch Pathol Lab Med. 2010;134:1210–1214. [PubMed: 20670145]
32. Kinney SN, Eble JN, Hes O, et al. Metanephric adenoma: the utility of immunohistochemical and cytogenetic analyses in differential diagnosis, including solid variant papillary renal cell carcinoma and epithelial-predominant nephroblastoma. Mod Pathol. 2015;28:1236–1248. [PubMed: 26248896]
33. Mantoan Padilha M, Billis A, Allende D, et al. Metanephric adenoma and solid variant of papillary renal cell carcinoma: common and distinctive features. Histopathology. 2013;62:941–953. [PubMed: 23551615]
34. Mehra R, Vats P, Cieslik M, et al. Biallelic Alteration and Dysregulation of the Hippo Pathway in Mucinous Tubular and Spindle Cell Carcinoma of the Kidney. Cancer Discov. 2016;6:1258–1266. [PubMed: 27604489]
35. The Cancer Genome Atlas Research N Linehan WM, Spellman PT, et al. Comprehensive Molecular Characterization of Papillary Renal-Cell Carcinoma. N Engl J Med. 2016;374:135–145. [PubMed: 26536169]
36. Zanconato F, Cordenonsi M, Piccolo S. YAP/TAZ at the Roots of Cancer. Cancer Cell. 2016;29:783–803. [PubMed: 27300434]
37. MacLennan GT, Farrow GM, Bostwick DG. Low-grade collecting duct carcinoma of the kidney: report of 13 cases of low-grade mucinous tubulocystic renal carcinoma of possible collecting duct origin. Urology. 1997;50:679–684. [PubMed: 9372874]
38. Peckova K, Martinek P, Sperga M, et al. Mucinous spindle and tubular renal cell carcinoma: analysis of chromosomal aberration pattern of low-grade, high-grade, and overlapping morphologic variant with papillary renal cell carcinoma. Ann Diagn Pathol. 2015;19:226–231. [PubMed: 26009022]
39. Chen YB, Xu J, Skanderup AJ, et al. Molecular analysis of aggressive renal cell carcinoma with unclassified histology reveals distinct subsets. Nat Commun. 2016;7:13131. [PubMed: 27713405]
40. Alexiev BA, Burke AP, Drachenberg CB, et al. Mucinous tubular and spindle cell carcinoma of the kidney with prominent papillary component, a non-classic morphologic variant. A histologic, immunohistochemical, electron microscopic and fluorescence in situ hybridization study. Pathol Res Pract. 2014;210:454–458. [PubMed: 24702883]

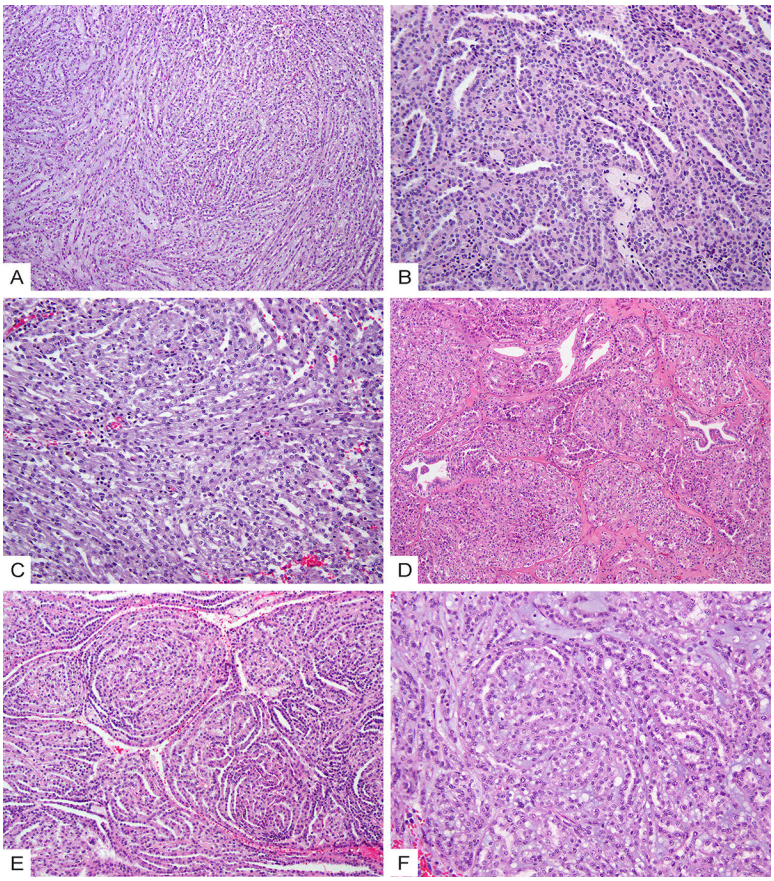

Figure 1.

Morphologic spectrum of mucinous tubular and spindle cell carcinoma (MTSCC). (A) Intermixed elongated tubules, spindle cells and stromal mucin; (B) short tubules and scattered foci of foamy macrophages; (C) spindle cells; (D) Solid areas and rare foci of papillations; (E) Compact arrangement of whorled, elongated tubules forming micronodules; (F) Whorled short tubules forming glomeruloid structures.

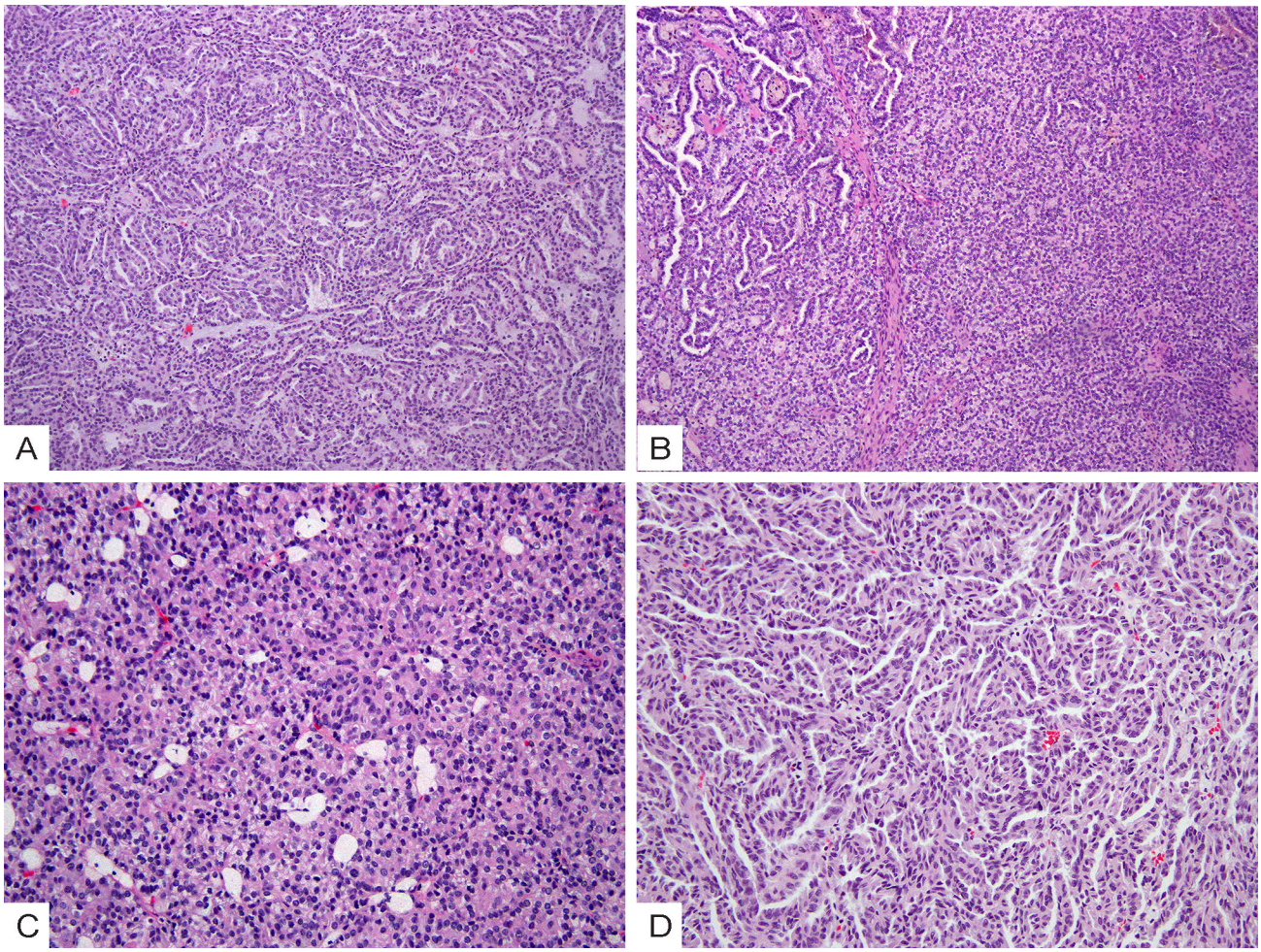

Figure 2.

Morphologic spectrum of solid variant of papillary renal cell carcinoma (PRCC). (A) Glomeruloid micronodules and abortive papillae; (B) Solid sheets of cells with scattered tubules (right) and a distinct area of well-formed papillae with type 1 PRCC histologic features (left); (C) Compact arrangement of ill-formed tubules with intermixed foamy macrophages; (D) Low-grade spindle cells lining angulated, curvilinear tubules with irregular and “shaggy” lumina.

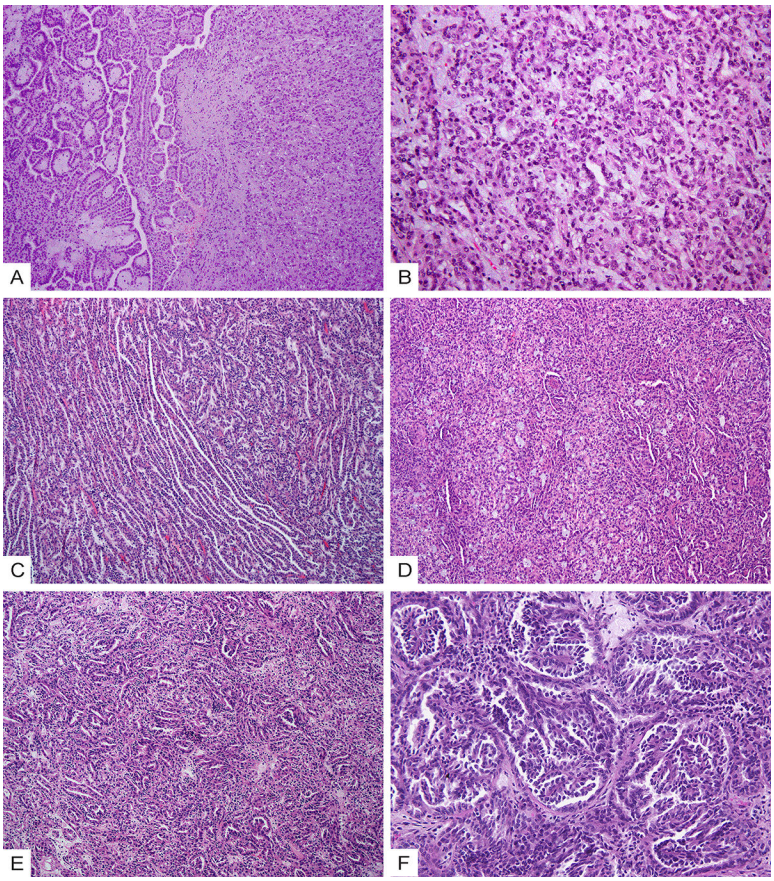

Figure 3.

Morphologic spectrum of indeterminate cases (IND) with overlapping features of MTSCC and PRCC. (A) A subset of cases show a distinct papillary region with well-formed papillae of type 1 PRCC (left) and MTSCC-like areas with intermixed tubules, spindle cells and stromal mucin (right). (B) High-power view of the MTSCC-like areas in (A). (C) Case IND4 shows areas with intermixed elongated tubules and abortive papillae. (D) Case IND7 shows intermixed tubular, solid and spindle cell components as well as mucin. (E) Intermixed tubules and micronodules. (F) Micronodules encompassing small branching papillae that have fibrovascular cores.

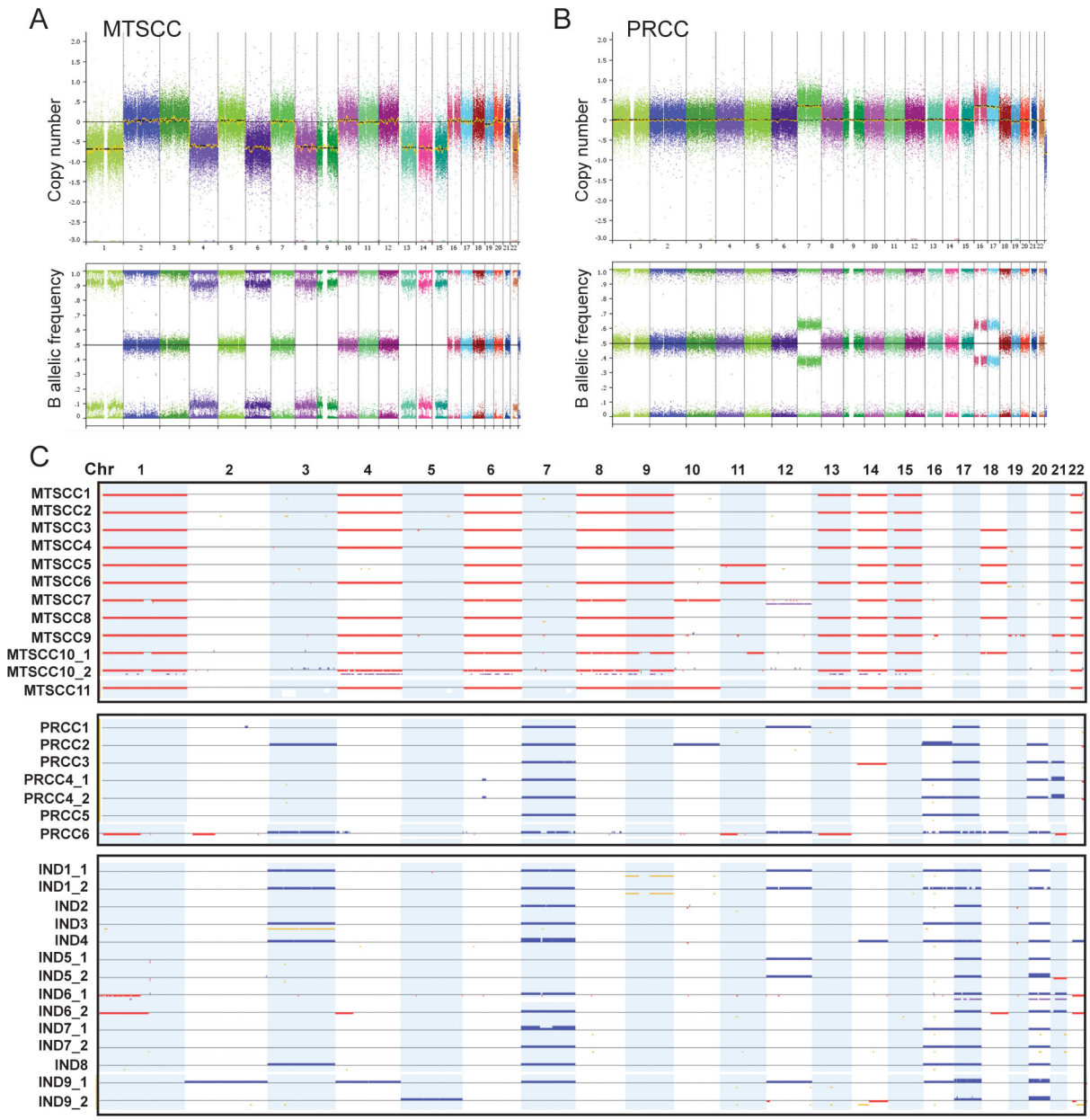

Figure 4.

SNP-array analysis of MTSCC, PRCC and IND cases. (A-B) Genome-wide view of copy number (CN) (top panel) and B allele frequency (BAF) (bottom panel) results from representative MTSCC (A) and PRCC (B) cases. All chromosomes are color-coded, and tracks consist of dots, which are calculated CN or BAF values at corresponding SNP positions. (C) Heat map of SNP-array results for all cases (n=26). Copy number gains (blue), losses (red), and copy-neutral loss of heterozygosity (CN-LOH, yellow) are displayed for each sample (rows) with chromosomes organized in columns and indicated by labels on the top. For 7 cases, there are two independent samples from the same tumor that are marked as "_1" and "_2".

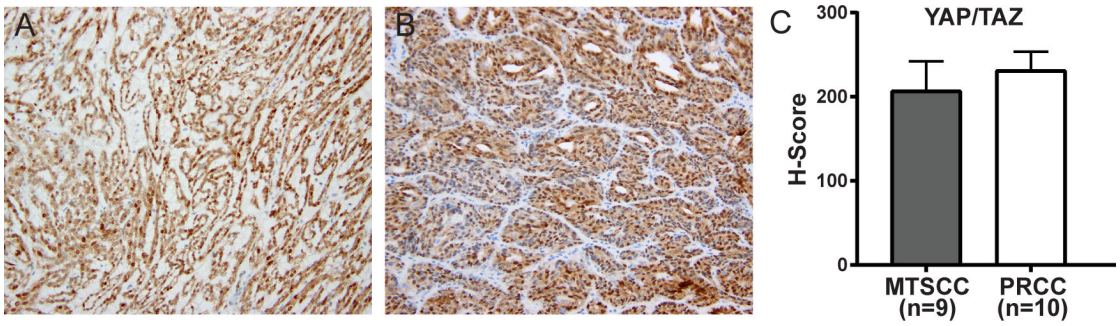

Figure 5.

Activation of Hippo-YAP signaling reflected by YAP/TAZ immunohistochemical staining. (A) Representative image of YAP/TAZ nuclear staining in MTSCC. (B) Representative image of YAP/TAZ nuclear staining in PRCC. (C) Immunostaining scores (H-scores) for YAP/TAZ nuclear staining were determined and presented as a bar graph on MTSCC (n=9) or PRCC (n=10) tumors. H-Scores [H= intensity (0–3) x percentage of positive cells (1–100)]. Bars, mean values; error bars, 95% C.I.

Table 1.

Summary of clinicopathologic features of 3 diagnostic groups

	MTSCC (n=11)	PRCC (n=6)	IND (n=9)
Age *	61 (21–74)	61 (56–74)	63 (41–74)
Gender			
Male	2 (18%)	5 (83%)	7 (78%)
Female	9 (82%)	1 (17%)	2 (22%)
Nephrectomy			
Partial	7 (64%)	4 (67%)	8 (89%)
Total/Radical	4 (36%)	2 (33%)	1 (11%)
Tumor size (cm) *	4.2 (1.3–16.5)	2.35 (1.4–9.5)	3.5 (1–16)
T stage (at nephrectomy)			
pT1	7 (64%)	5 (83%)	6 (67%)
pT2	4 (36%)	1 (17%)	2 (22%)
pT3	0	0	1 (11%)
Regional lymph nodes (at nephrectomy)			
Nx/N0	11 (100%)	6 (100%)	9 (100%)
Distant metastases (during follow-up)			
M0	11 (100%)	6 (100%)	8 (89%)
M1	0	0	1 (11%)
Papillary adenoma(s)	1 (9%)	0	3 (33%)
Follow-up (month) *	46 (3–88)	27 (4–91)	57 (19–120)
Deaths (n)	0	0	0

*Median (range)

MTSCC, mucinous tubular spindle cell carcinoma; PRCC, solid variant of type 1 papillary renal cell carcinoma; IND, indeterminate cases with overlapping histologic features of MTSCC and PRCC.

Table 2.

Morphologic features of MTSCC, PRCC, and IND cases (n=26)

Case #	Capsule	Elongated tubules (%)	Short tubules (%)	Spindle cells (%)	Solid sheets (%)	Micronodules/abortive papillae (%)	Well-formed papillae (%)	Mucin	Foamy macrophages
MTSCC1	Yes	80	0	10	0	10	0	Apparent	Not apparent
MTSCC2	No	70	5	20	0	5	rare foci (<1%)	Apparent	Not apparent
MTSCC3	Yes	60	20	0	10	10	0	Apparent	Not apparent
MTSCC4	No	20	40	20	15	5	0	Apparent	Present
MTSCC5	No	50	20	10	15	5	0	Poor	Present
MTSCC6	Yes	30	20	25	20	5	0	Apparent	Present
MTSCC7	Yes *	10	30	20	30	10	rare foci (<1%)	Poor	Present
MTSCC8	Yes	40	20	30	0	10	0	Apparent	Present
MTSCC9	Yes	80	10	10	0	0	0	Apparent	Present
MTSCC10	No	50	10	10	20	10	rare foci (<1%)	Poor	Present
MTSCC11	No	30	35	20	10	5	rare foci (<1%)	Poor	Not apparent
PRCC1	Yes	0	40	0	50	0	10	No	Abundant
PRCC2	Yes *	0	0	30	10	60	0	No	Not apparent
PRCC3	Yes *	10	35	10	40	5	rare foci (<1%)	No	Abundant
PRCC4	Yes	5	5	10	20	50	10	No	Abundant
PRCC5	No	20	5	0	25	30	20	No	Abundant
PRCC6	No	10	0	0	5	80	5	No	Not apparent
IND1	Yes	30	20	10	10	30	rare foci (<1%)	Focal	Present
IND2	No	20	10	0	50	20	rare foci (<1%)	Poor	Not apparent
IND3	Yes	40	5	10	0	40	5	Poor	Present
IND4	No	30	20	10	0	40	0	No	Present
IND5	No	5	20	0	30	5	40	Apparent	Present
IND6	No	10	5	20	20	10	35	Apparent	Present
IND7	Yes *	10	35	0	40	10	5	Present (luminal)	Not apparent
IND8	No	10	20	10	0	55	5	Poor	Present
IND9	Yes *	10	5	10	60	5	10	No	Abundant

* Fibrous capsule is present but only partially surrounding the tumor.

Table 3.

Morphologic features identified in PRCC but not MTSCC

Morphologic features	MTSCC (n=11)	PRCC (n=15)	Illustration	P-value (Fisher-exact)
Distinct area of type 1 PRCC	0	6 (40%)	Fig. 2B; 3A	**0.02** *
Low-grade spindle cells lining tubules with irregular and “shaggy” lumina	0	6 (40%)	Fig. 2D	**0.02** *
Micronodules encompassing small papillae	0	2 (13%)	Fig. 3F	0.5

* $p < 0.05$

Table 4.

Immunohistochemical features between MTSCC and PRCC

	CD10	CK7	AMACR	CD15	Pax8	EMA
MTSCC	3/10 (30%)	10/10(100%)	10/10 (100%)	6/10 (60%)	10/10 (100%)	9/10 (90%)
PRCC	9/13 (69%)	13/13 (100%)	13/13 (100%)	7/10 (70%)	13/13 (100%)	8/10 (80%)